Rotational seismograms on the Moon

David Sollberger[1], Cedric Schmelzbach[1], Johan O. A. Robertsson[1], Stewart Greenhalgh[1], Yosio Nakamura[2], Amir Khan[1]
[1]**Institute of Geophysics, ETH Zurich, Switzerland;** [2]Institute for Geophysics, University of Texas at Austin, USA

ETH zürich

1 Introduction

The Apollo missions included a range of **active and passive seismic** experiments that aimed to explore and characterize the lunar subsurface below the landing sites. During the Apollo 17 mission, astronauts employed explosive packages on the lunar surface (Figure 1). The resulting seismic response was recorded by a triangular array of vertical-component geophones (Figure 2).

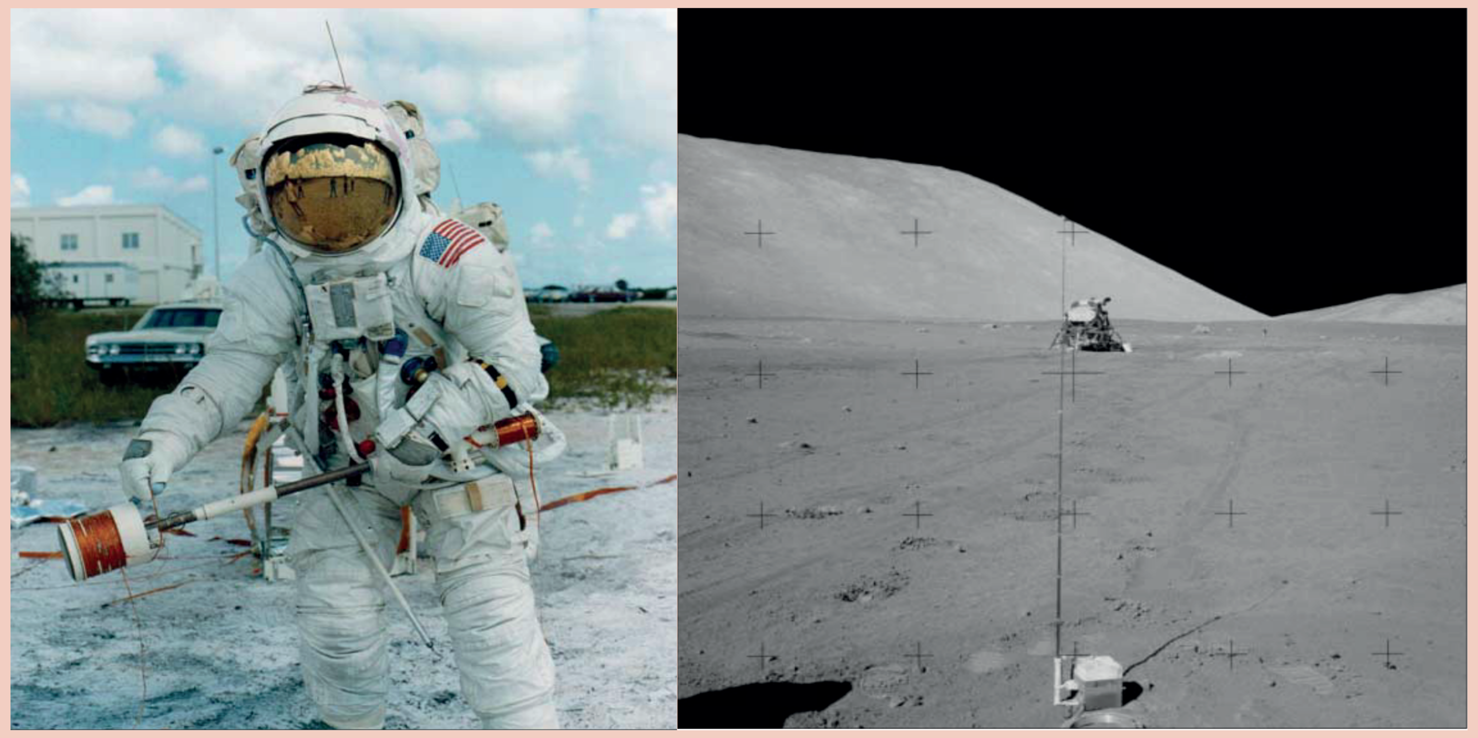

Figure 1: Left: Apollo backup astronaut training with a seismic thumper source. Right: Explosive package employed on the lunar surface during the Apollo 17 mission. ©NASA

Scope of this study:

- Application of **spatial wavefield gradient analysis** to the Apollo 17 lunar seismic profiling experiment (LSPE) data
- Analysis of wavefield gradients yield key parameters such as apparent **phase velocity and rotational ground motion**
- **S-wave arrivals** are identified based on their lower apparent phase velocity and distinct higher amount of rotational motion relative to P-waves.

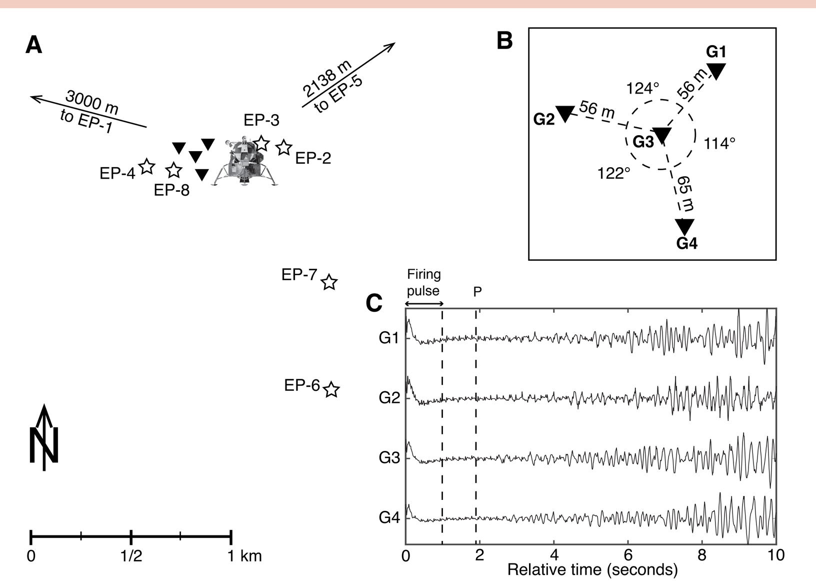

Figure 2: The Apollo 17 lunar seismic profiling experiment (LSPE). **A)** Map of LSPE showing the locations of the four geophones (black triangles), the eight explosive packages (stars), and the lunar module (pictogram). **B)** Detailed view of the geophone configuration. **C)** Data recorded at the four geophones as a response to firing of EP-7.

2 Shear wave identification

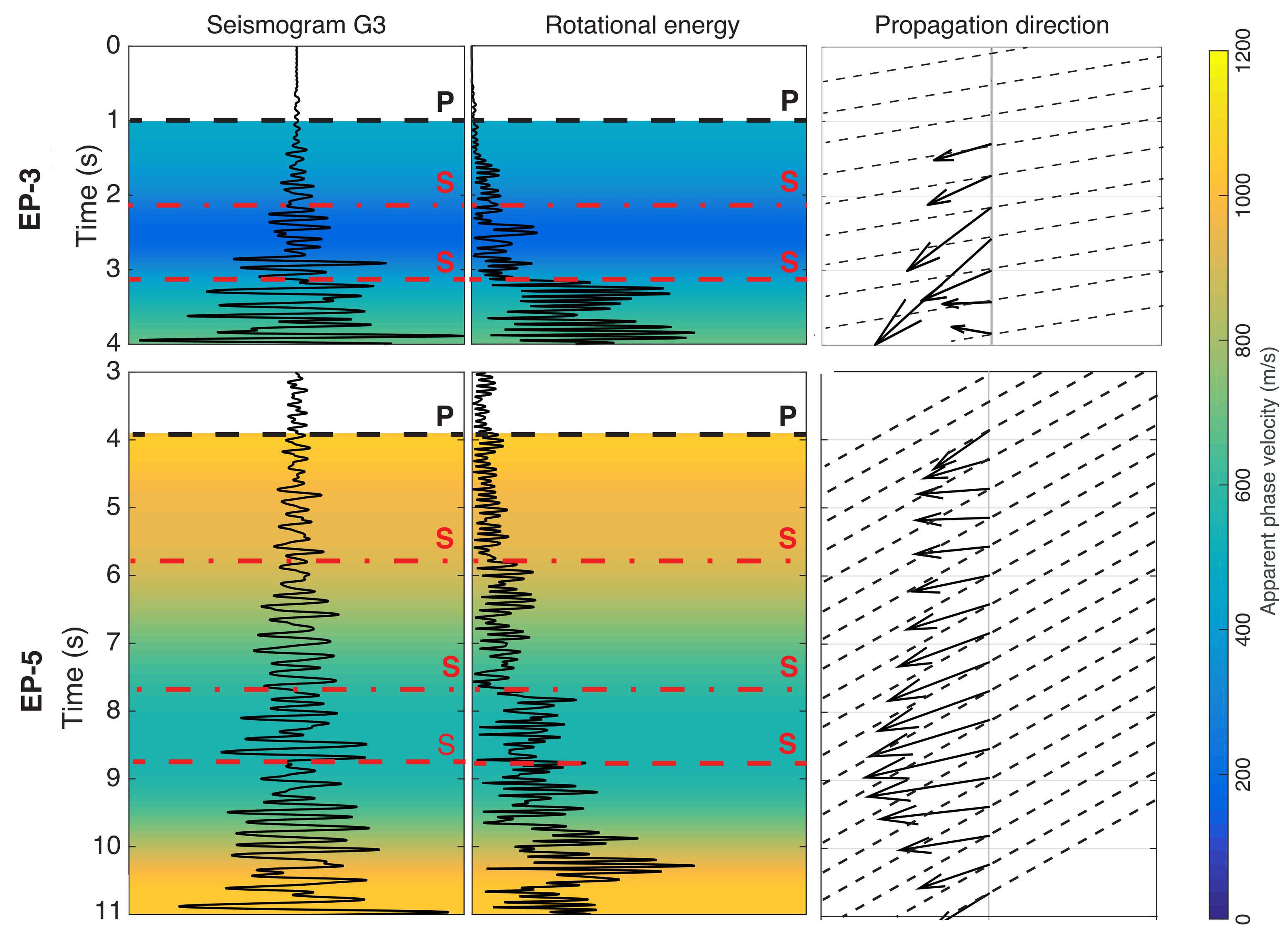

Figure 3: Gradient-based estimates of apparent phase velocity, rotational ground motion, and propagation direction as a function of time, shown for EP's 3 and 5. Identified shear wave arrivals are marked in red. Rotational energy corresponds to summed energy of the two horizontal components of rotation (tilts) that are estimated by spatial gradient analysis. Dashed lines underlying the propagation direction estimates mark the source-receiver azimuth according to the survey geometry (Figure 2).

3 Seismic velocity structure of the lunar crust

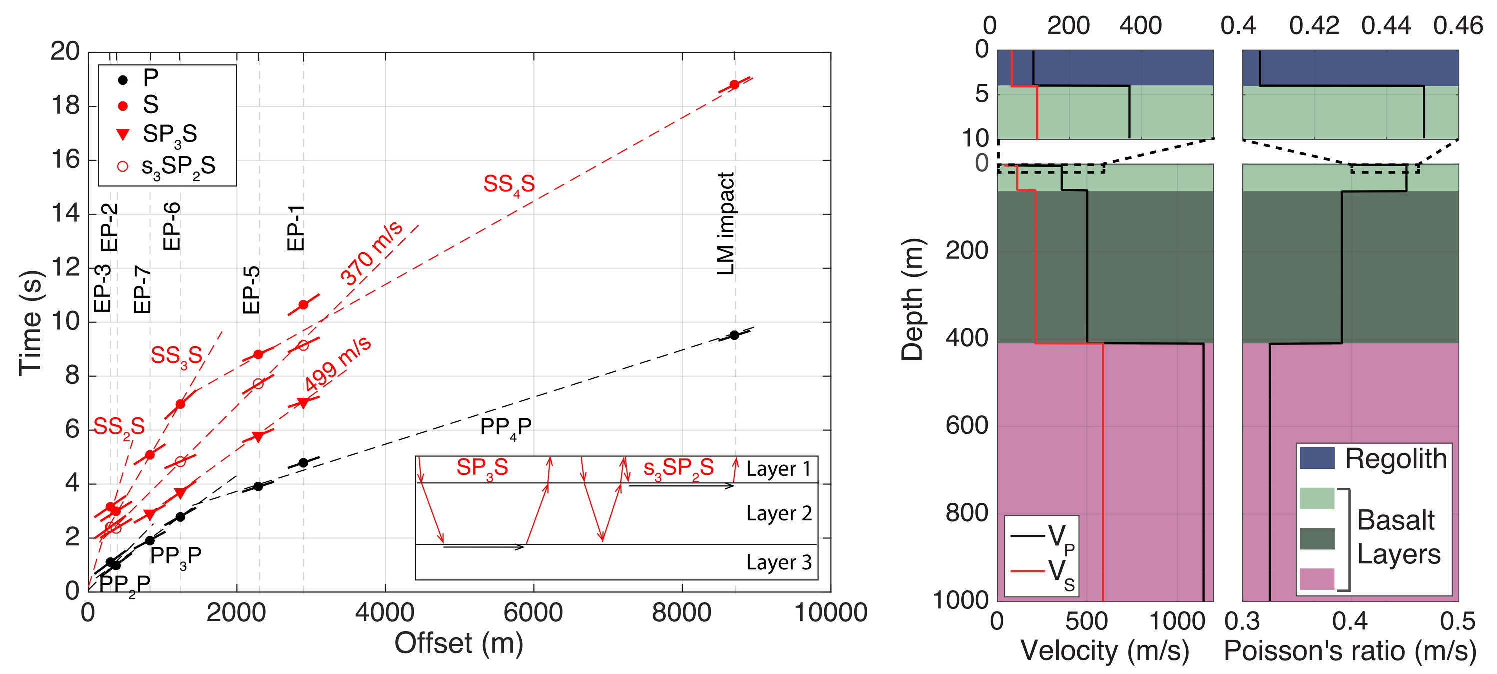

Figure 4: Extracted traveltime curves for P- and S-waves. The slope of the solid lines going through each pick corresponds to the apparent phase velocity that was estimated by spatial gradient analysis. Dashed lines indicate predicted travel times for different refracted modes using standard modeling of critically refracted arrivals in a layered medium and our preferred velocity model of the lunar near-surface structure, shown on the right.

4 Comparison to synthetics

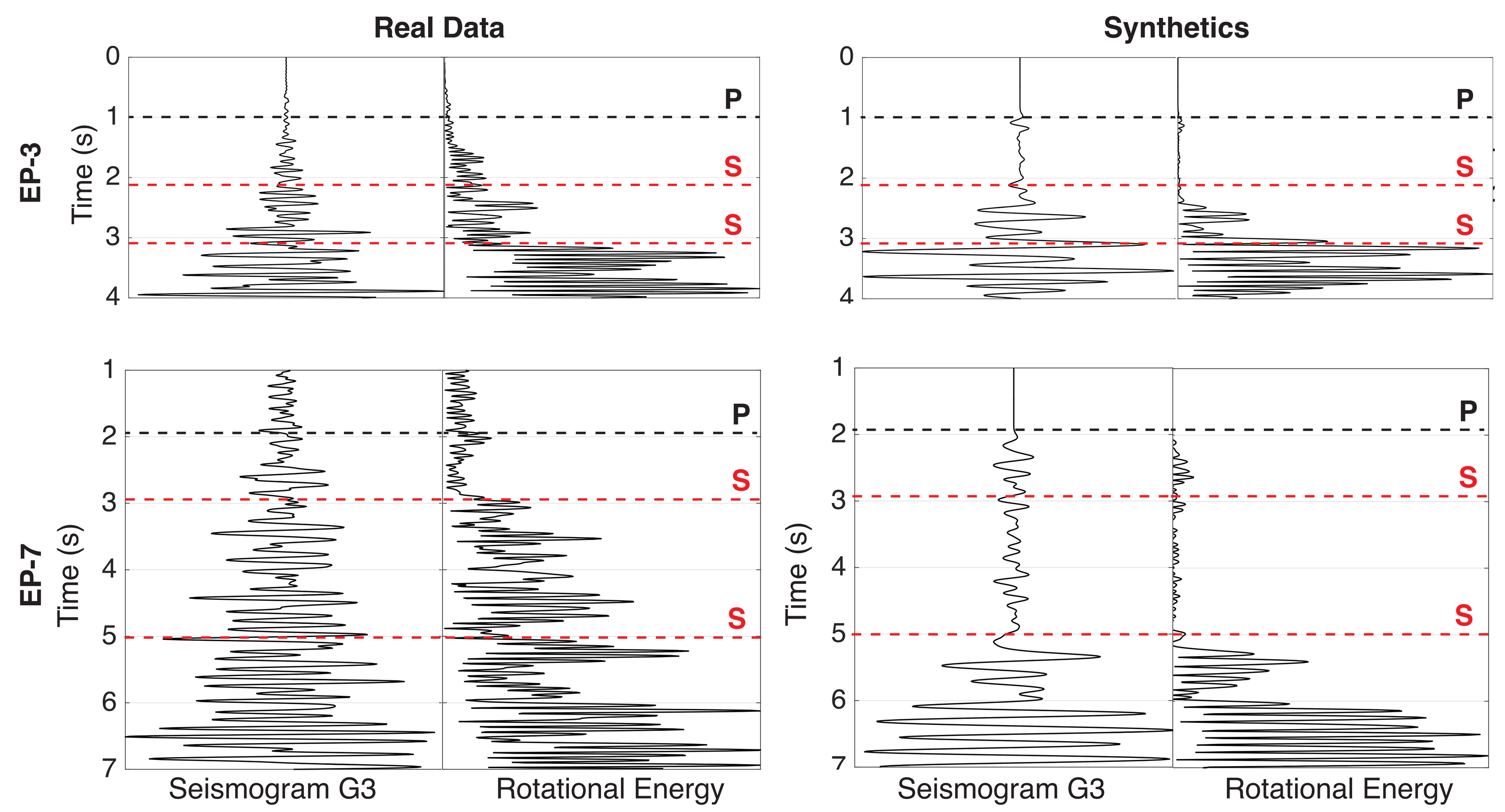

Figure 5: Left: vertical-component seismograms and array-derived rotational ground motion of the Apollo 17 LSPE data. Results are shown for EP's 3 and 7. Right: synthetic vertical-component seismograms and corresponding rotational ground motion for EP's 3 and 7 obtained by finite-difference modelling using our preferred velocity model (Figure 4). Note that shear wave arrivals are associated with a distinct higher amount of rotational energy in both the real and synthetic data, yielding this observable a useful diagnostic to identify shear wave arrivals in complex seismic data.

5 Conclusions

- Array-based estimates of rotational ground motion and apparent phase velocity highly facilitate the identification of shear-wave arrivals on seismic data
- First seismic shear-wave velocity profile of the shallow lunar crust
- Given the rich information derived from the minimalistic recording configuration, our results demonstrate that **rotational seismometers should be critically considered for future space missions** that aim to explore the interior structure of extraterrestrial objects by seismic methods.

CARNEVAL industry consortium

Schlumberger OMV nagra